Investigation of Fuel Cell Anode at Higher Temperature with Reformate Fuel by AC Impedance Spectroscopy

Ruichun Jiang, H. Russell Kunz, James M. Fenton
Department of Chemical Engineering, University of Connecticut, Storrs, CT 06269, USA

Abstract

In this work, *In-Situ* AC impedance based diagnostics of H_2 dissociative adsorption, oxidation, and CO poisoning were performed at higher temperatures (> 100°C) and ambient pressure conditions. Pt-Ru/C (ETEK, 40% wt., Pt/Ru=1/1) as the anode catalyst was studied by AC impedance at various cell temperatures, CO concentrations and relative humidities. The impedance spectrum of the poisoned anode was strongly dependent on cell temperature, relative humidity, CO concentration and DC bias potential. CO poisoning was alleviated by increasing the cell temperature. Pseudo-inductive behaviors were observed under certain DC bias potential conditions in the complex impedance plots, corresponding to the onset oxidation and removal of CO on the catalyst active surface.

Keywords

AC impedance; carbon monoxide (CO); anode catalyst; high temperature; fuel cell.

Introduction

The major impediment in the development of proton exchange membrane (PEM) fuel cells running on either industrial hydrogen (contaminated with carbon monoxide and other hydrocarbons) or hydrogen feed streams derived from carbon-based fuels (e.g., cracked or reformed methanol) arises from the dramatic deactivation of the anode electrocatalyst by even trace levels of CO.[1, 2] For low temperature fuel cell operating conditions (T_{cell} < 100ºC), due to the strong affinity between CO and Pt, CO adsorption on the catalyst blocks the reaction sites for hydrogen adsorption and oxidation, thus leading to serious CO poisoning.[1, 2, 3] Since CO adsorption on the catalyst is an exothermic reaction, CO coverage on the catalyst decreases with rising temperature. In our previous fuel cell performance study, operation of the fuel cell at higher temperature (105°C and 120°C) effectively reduced performance losses due to CO poisoning.[3] However, at higher temperatures and ambient pressure, the popularly used Nafion® membrane becomes dry and leads to a high resistance due to the low relative humidity at atmospheric conditions. To reduce the IR losses at higher temperature/ambient pressure conditions, Nafion® based composite membrane, Nafion®-Teflon®-$Zr(HPO_4)_2$ membrane was developed and applied in high temperature PEM fuel cells.[4] This membrane shows promising proton conductivity at higher temperature fuel cell operating conditions and makes the study of the CO tolerance properties of higher temperature/ambient pressure PEM fuel cells feasible.

AC impedance spectroscopy based techniques, can unravel different surface processes in its frequency domain, which is suitable for studying electrochemical processes on the catalyst surface. AC impedance has been used widely in some other electrochemical research fields such as corrosion and lithium ion batteries. In recent years, AC impedance has also proved useful in fuel cell research. As a diagnostic tool for characterizing fuel cell behavior, AC impedance can

determine the various sources of polarization losses in the frequency domain, which provides useful information for optimizing fuel cell design and operating conditions. The AC impedance spectroscopy of the fuel cell anode changes when CO is introduced into the H_2 stream. The separation in the frequency domain of the various rate processes contributing to overpotential can provide a better insight on the mechanistic aspects of CO poisoning. Impedance theories and models for fuel cells have also been developed to interpret catalytic activity losses due to CO poisoning. Almost all of the AC impedance studies before on CO poisoning of the anode were performed under lower temperature fuel cell operating conditions (< 100°C and 100% R.H.). In this study, the AC impedance based diagnostics of H_2 dissociative adsorption, oxidation and CO poisoning under higher temperature (> 100°C and < 100% RH) and ambient pressure conditions will be reported. Temperature, relative humidity, CO concentration as well as DC bias potential effects on AC impedance behaviors were investigated. The phenomena of pseudo-inductive behavior observed in the complex impedance plots under certain DC bias potentials can be rationalized with the "onset potential" for CO oxidation.

Experimental

The Nafion®-Teflon®-$Zr(HPO_4)_2$ membranes were developed by impregnating a Teflon® matrix with a solution containing Nafion® and $Zr(HPO_4)_2$, which was generated in-situ according to the reaction: $ZrOCl_2 + 2\ H_3PO_4 \rightarrow Zr(HPO4)_2 + 2\ HCl + H_2O$.[4] Catalyst inks were prepared by mixing and dispersing the carbon supported catalyst and Nafion® at a mass ratio of catalyst/Nafion® = 75/25 in methanol. 40 wt % Pt-Ru/C with Pt:Ru atomic ratio of 1:1 from E-TEK (Somerset, NJ) was used for the anode catalyst and 46.8 wt % Pt/C (Tanaka, Kikinzoku Kogyo K.K. Japan) was used for the cathode. The membrane electrode assembles (MEAs) were prepared by spraying catalyst ink containing carbon-supported catalyst and Nafion® in methanol onto the membrane.

The AC impedance spectroscopy measurements were carried out with MEAs in a two-electrode arrangement to enable a direct extrapolation of data to fuel cell conditions. using a Solartron (Houston, TX) 1250 frequency response analyzer together with the Solartron 1287 electrochemical interface. The experiments were controlled and with data recorded using ZPLOT impedance software (Scribner Associates, Inc., Southern Pines, NC) at 80°C and 120°C under atmospheric pressure. The gas flow rate was controlled using a Scribner 890B fuel cell test system load box (Scribner Associates, Inc., Southern Pines, NC). For the 80°C and 120°C cell temperature operation, the humidification temperature was kept at 90°C for both the anode and cathode for inlet relative humidification of 100% and 35%, respectively. AC impedance was carried out by applying a small alternating voltage (10-50 mV) to the anode at a constant DC voltage by varying the frequency of the alternating voltage from 1×10^5 Hz to 0.01 Hz. AC impedance measurements were first performed with a H_2/H_2 cell. The behavior of the poisoned electrode was subsequently studied in H_2+CO/H_2 cells, in which the gas in the working compartment was switched to gas mixtures with different CO content (100 ppm and 2% CO +24% CO_2).

Results and Discussions

AC impedance at open circuit voltage (OCV). The AC impedance was first operated in a two-electrode cell arrangement at the open cell voltage (OCV). Pure H_2 or H_2 with different levels of CO was applied to the cell anode which used as the working electrode; pure H_2 was used in the cell cathode which also acted as the reference and counter electrode. The complex impedance plots obtained at OCV under different temperature and different CO concentrations are presented in

Figure 1, Figure 2 and Figure 3. The complex impedance plots are flatted semicircles with the high frequency (HF) end on the left side and the low frequency (LF) end on the right side. According to Ciureanu *et. al.*,[5] for anodic oxidation of H_2 and H_2 containing CO, the flatted semicircle is made of two arcs, which often overlap each other and are not easily distinguished. The two arcs in the complex impedance plots are formed due to the equilibrium processes occurring at the reaction interface. The arc at the high frequency region is due to the reversible charge transfer process involving the adsorbed hydrogen atoms ($H_{ads} = H^+ + e^-$); the arc at lower frequencies is associated with the polarization impedance, due to the dissociative chemisorption of hydrogen ($H_2 = 2H_{ads}$).[5] The impedance at the intersection of the HF curve (left side intersection) with the real axis is attributed to the internal resistance of the cell, R_1 (or R_{HF}), which is assigned as the cell resistance. The distance between the HF and the LF intersection points of the spectra with the real axis (R_{LF}-R_{HF}) is governed by both the charge transfer resistance and the adsorption resistance. Figure 1 and Figure 2 show that with pure H_2 applied in the cell anode, the complex impedance plots at 120°C (35% RH) have similar shape, but larger curves compared with that at 80°C (100% RH). The lower relative humidity at the higher temperature operation causes dehydration of the cell membrane and ionomer inside the catalyst layer. The ion transfer resistance in the electrode increases as well as the membrane resistance. Therefore, the intersections on the real axis of the HF curve shift to higher values due to higher membrane resistance. The distance between the intersection of the HF and LF curves on the real axis increased due to larger ion transfer resistance in the electrode. Figure 1 and Figure 2 also compare the impedance data using H_2 with 100 ppm CO in the anode. In each temperature condition, the impedance curve size increases when CO is introduced in the cell. In view of considerable changes observed with respect to the symmetrical H_2/H_2 cell, it may be inferred that the impedance of the cell is mostly due to CO poisoning of the anode working electrode. At each operation temperature condition, the values of HF intersections with the real axis are similar under different fuel compositions. The CO poisoning effects can be compared qualitatively by comparing the LF intersection values of H_2 with CO, $R_{LF\ H2+CO}$, and pure H_2, $R_{LF\ H2}$, ($\Delta R_{LF} = R_{LF\ H2+CO} - R_{LF\ H2}$). It is obviously that the value of ΔR_{LF} is smaller at 120° than that at 80°C, indicating that higher temperature has better CO tolerance. Figure 3 compares the AC impedance plots at 80°C and 120°C with 2%CO+24%CO_2 in H_2 as the anode fuel. With higher CO concentrations applied, the impedance curves increase greatly comparing with pure H_2 condition. Impedance at 80°C is much larger than that at 120°C with 2% CO in the fuel. Adsorption of CO on the electrode surface increases significantly with higher CO concentrations; therefore, the H_2 dissociative adsorption impedance increases. CO adsorption on the Pt based alloy catalyst surface is exothermic, higher temperature operation reduces CO coverage of the anode electrode catalyst; therefore, the impedance curve size of the LF arc associated with H_2 adsorption decreases with increasing temperature.

AC impedance with bias potentials. Figure 4 shows the bias potential effects on impedance plots at 120°C (35% RH) with 2%CO+24%CO_2 in H_2. The impedances with low potentials (0.05-0.4V) are similar with that at OCV, but the LF impedance spectrum increases with increasing potentials. When a DC bias potential was applied, a corresponding DC bias current occurred in the system, this current cause more hydrogen molecules to be absorbed and react than at OCV; however, the low value of this potential does not reach the onset potential for CO oxidation and a big part of the electrode surface is still occupied by CO. The impedance for hydrogen adsorption is increased with bias potential in this low potential range. When a higher bias potential (> 0.6V) is applied, the impedance spectrum pattern at LF changes. The diameter of the impedance curve becomes smaller and a small loop appears in the fourth quadrant of the complex plane diagram,

i.e., a typical pseudoinductive behavior. Such patterns are characteristic for systems with consecutive heterogeneous reactions with adsorbed intermediates, or for showing a transition between passive and active states.[5-9] Conway *et al*.[7] have demonstrated that a semi-inductive behavior in systems with adsorbed species is associated with a change in the sign of the coverage dependence on potential. Ciureanu *et al*.[5] also described this phenomenon in their study with a fuel cell at 50°C and 75°C. This pseudoinductive phenomenon can be attributed to CO oxidation by oxygenated species on the electrode surface resulting in a dynamic state of CO adsorption-oxidation and removal-readsorption. The CO coverage starts decreasing at this potential due to oxidation removal which activates the surface for subsequent hydrogen chemisorption.

Conclusions

Higher impedance was observed at the LF intercept with higher CO concentrations due to less CO free electrode active surface for hydrogen adsorption. Higher temperature complex plots show smaller ΔR_{LF} in impedance curves for each CO concentration than at low temperature conditions, 80°C. CO poisoning was reduced at high temperature due to CO's exothermal adsorption reaction mechanism, therefore, more vacant active surface sites were available for hydrogen adsorption, induced lower impedance for hydrogen chemisorption characteristic at low frequency. Impedance spectra changed when a bias DC potential was applied. At a specific temperature and CO concentration, as the bias DC potential increased, the impedance increased due to a higher hydrogen oxidation over potential. When the bias potential is higher than the CO oxidation onset potential, a psudoinductive curve appears in the fourth quadrant, indicating the beginning of CO oxidation and removal from the anode electrode.

Reference:

1. S. Gottesfeld, T. A. Zawodzinski, Polymer Electrolyte Fuel Cells, Advances in Electrochemical Science and Engineering, Vol. 5, 1997, WILEY-VCH.
2. R. Jiang, Y. Si, J. Lin, H. R. Kunz, J. M. Fenton, Abstracts of the 203rd Meeting of Electrochemical Society, Paris, May. 2003. (Abstract No. 176)
3. Y. Si, R. Jiang, H. R. Kunz, J. M. Fenton, *J. Electrochemical Society,* **151(11)**, 1 (2004).
4. Y. Si, H. R. Kunz, and J. M. Fenton, *J. Electrochem. Soc*., **151(4)**, A623 (2004).
5. (a). M. Ciureanu, H. Wang, *J. Electrochem. Soc.*, **146**, 4031 (1999); (b). M. Ciureanu, H. Wang, Z. Qi, *J. Phys. Chem.* B. **103**, 9645 (1999).
6. (a). R. D. Armstrong, *Electroanal. Chem.* **34**, 387 (1972). (b). R. D. Armstrong and M. Henderson, *J. Electroanal. Chem.* **39**, 81 (1972).
7. M. Keddam O. R. Mattos and H. Takenouti, *J. Electrochem. Soc*., **128**, 257 (1981).
8. L. Bai and B. E. Conway, *J. Electrochem. Soc*., **137**, 3737 (1990).
9. L. J. Gao and B. E. Conway, *J. Electroanal. Chem*., **395**, 261 (1995).

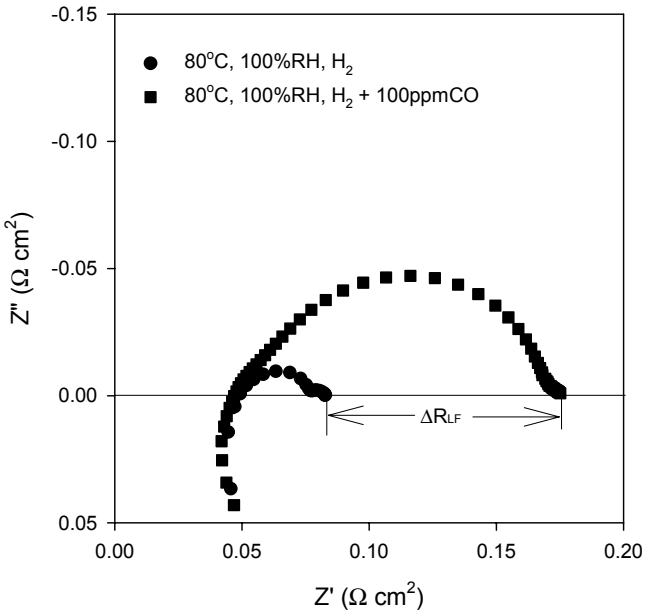

Figure 1. Complex impedance plots of 40 wt % Pt-Ru/C (Pt/Ru = 1/1) using pure H_2 and H_2 with 100 ppm CO in the anode at OCV and 80°C (100% RH).

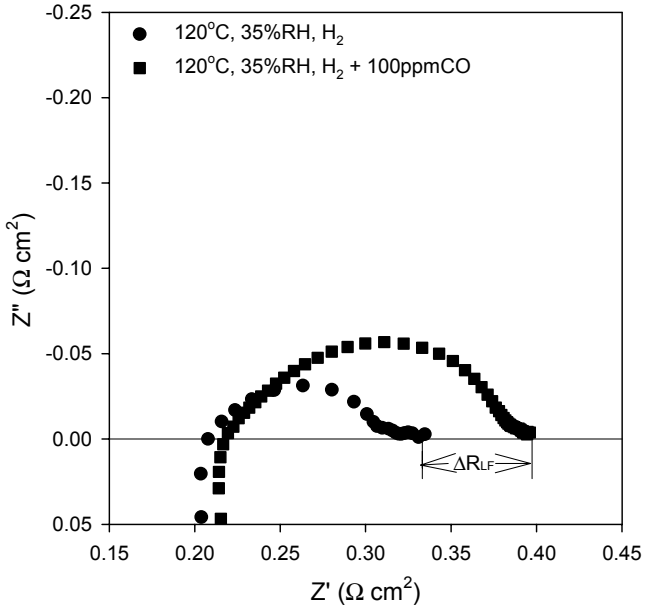

Figure 2. Complex impedance plots of 40 wt % Pt-Ru/C (Pt/Ru = 1/1) using pure H_2 and H_2 with 100 ppm CO in the anode at OCV and 120°C (35% RH).

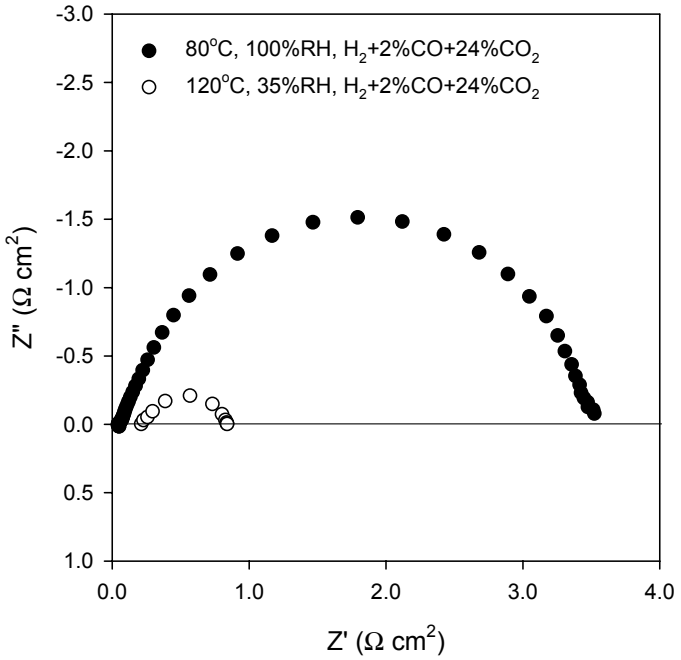

Figure 3. Complex impedance plots of 40 wt % Pt-Ru/C (Pt/Ru = 1/1) using H_2 with 2%CO+24%CO_2 in the anode at OCV, 80°C (100% RH).and 120°C (35% RH).

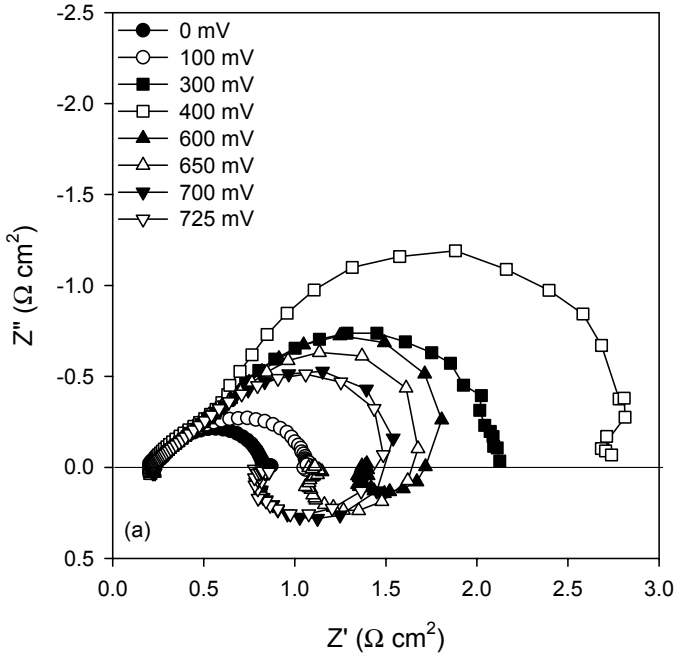

Figure 4. Impedance plots of 40 wt % Pt-Ru/C (Pt/Ru = 1/1) in a H_2+2%CO+24%CO_2/H_2 cell at various bias potentials under 120°C (35% RH).